

## Review

# A Review of Bubble Aeration in Biofilter to Reduce Total Ammonia Nitrogen of Recirculating Aquaculture System

Putu Ayustin Suriasni <sup>1</sup>, Ferry Faizal <sup>1,2</sup> , Camellia Panatarani <sup>1,2</sup>, Wawan Hermawan <sup>2,3</sup> and I Made Joni <sup>1,2,\*</sup> 

<sup>1</sup> Department of Physics, Faculty of Mathematics and Natural Science, Padjadjaran University, Jl. Raya Bandung-Sumedang KM 21, Sumedang, West Java 45363, Indonesia

<sup>2</sup> Functional Nano Powder (FiNder) University Center of Excellence, Padjadjaran University, Jl. Raya Bandung-Sumedang KM 21, Sumedang, West Java 45363, Indonesia

<sup>3</sup> Department of Biology, Faculty of Mathematics and Natural Science, Padjadjaran University, Jl. Raya Bandung-Sumedang KM 21, Sumedang, West Java 45363, Indonesia

\* Correspondence: imadejoni@phys.unpad.ac.id

**Abstract:** Aeration becomes an essential aspect of biofilter performance to reduce ammonia nitrogen in the Recirculating Aquaculture System (RAS). Efficient aeration introduces air into water media and offers an aerobic environment in the biofilter for microbial degradation of organic matter and ammonia nitrogen. The efficiency of the bubble aeration depends on the size of the bubbles; these include coarse bubble, microbubble, fine bubble, and ultrafine bubble or nanobubble. This review highlights an overview of bubble aeration features in a biofilter to reduce ammonia nitrogen. Moreover, key aspects responsible for the ammonia nitrogen removal efficiencies, such as oxygen transfer, microbial community, and biofilm thickness, are evaluated in this review. In conclusion, the bubble size of aeration affects the microbial community of nitrifying bacteria, consequently determining the growth and thickness of biofilm to improve ammonia removal efficiency. It is emphasized that fine bubble and nanobubble aeration have very positive prospects on improving biofilter performance, though they are currently not widely used in RAS.



**Citation:** Suriasni, P.A.; Faizal, F.; Panatarani, C.; Hermawan, W.; Joni, I.M. A Review of Bubble Aeration in Biofilter to Reduce Total Ammonia Nitrogen of Recirculating Aquaculture System. *Water* **2023**, *15*, 808. <https://doi.org/10.3390/w15040808>

Academic Editors: Marco Pellegrini, Cesare Sacconi, Alessandro Guzzini and José Alberto Herrera-Melián

Received: 28 October 2022

Revised: 16 February 2023

Accepted: 17 February 2023

Published: 19 February 2023



**Copyright:** © 2023 by the authors. Licensee MDPI, Basel, Switzerland. This article is an open access article distributed under the terms and conditions of the Creative Commons Attribution (CC BY) license (<https://creativecommons.org/licenses/by/4.0/>).

**Keywords:** aeration; biofilter; RAS; bubble

## 1. Introduction

In recent years, the RAS has become extensively applied in aquaculture production to decrease the impact of wastewater pollution on the environment [1]. The RAS is a closed aquaculture system that reuses water by replacing water volume by less than 10% [2]. Water replacement is conducted through recirculation and implementing various treatments to reduce contaminants in the wastewater. Wastewater is polluted water generated from industrial processes, including aquaculture waste. Therefore, wastewater treatment must remove the contaminants and leave an effluent with a less negative impact on aquaculture and the environment. The stages broadly incorporate physical, biological, and chemical processes that take place in that order. The first stage is primary treatment using a physical process such as sedimentation and flotation to remove organic and inorganic solids. The second stage is secondary treatment using a biological process to transform pollutants into stable forms through oxidation or nitrification. Finally, the third stage is tertiary treatment using a chemical process to remove specific wastewater pollutants that are unresolved from secondary treatment [3,4].

Ammonia nitrogen is a critical process parameter to be controlled in the RAS, which strongly affects the health and growth of aquaculture species [5]. Therefore, introducing effective and efficient wastewater treatments is very crucial in RASs. A biofilter is one of the methods in RAS wastewater treatments. Efficient aeration enables the introduction of air into the water media, offering an aerobic environment as a biofilter for microbial degradation of contaminants such as ammonia nitrogen. Therefore, aeration becomes

essential in aerobic biofilters where enhanced dissolved oxygen probably improves organic degradation performance. However, when selecting an aeration system, it is also needed to consider its energy usage. The advantages of advanced aeration technology offer multiple economic and environmental benefits, correspondingly reducing operating costs and energy savings. Therefore, recent aeration technology needs to consider implementing low-carbon technology in line with the demand of every nation to meet net-zero carbon emissions goals [6]. It means that a reliable biofilter with efficient aeration contributes to energy-saving solutions and cutting greenhouse gas emissions. Thus creating affordable, sustainable, long life-cycle and high-performance biofilters is the next urgently needed and significant challenge.

Based on the growth of the microorganisms, biofilters classify as suspended growth or fixed film [7]. In the suspended growth system, heterotrophic bacteria remain suspended in the water through stirring [8]. On the other hand, in an attached growth system or fixed film, autotrophic bacteria attach to a solid surface, such as rock, sand, metal, and plastic [9]. One of the most common fixed film bioreactors in an RAS is a Moving Bed Biofilm Bioreactor (MBBR). An MBBR utilizes small floating plastic media to serve as a surface for bacterial attachment and biofilm growth [10]. Furthermore, under aerobic conditions, nitrification occurs in biofilm when Total Ammonia Nitrogen (TAN) oxidizes into nitrite ( $\text{NO}_2^-$ ) and nitrate ( $\text{NO}_3^-$ ) [11]. Another example of the bioreactor in the RAS is the Biological Aerated Filter (BAF). The biofilm formed in the BAF reactor contains aerobic and anaerobic layers, which guarantee biomass structure stability and contaminant degradation [12].

The essential factors that influence biofilter performance are mass transfer and oxygen distribution. First, dissolved oxygen (DO) is responsible for enhancing biofilm growth and, consequently, TAN degradation through nitrification [13]. The mass or oxygen transfer from DO in the water to biofilm depends on many factors, such as biomass concentration, aeration rate, hydrodynamic condition, and biofilm characteristics [14]. Therefore, an aeration system with natural or mechanical aeration is usually utilized to provide a sufficient amount of DO for the biofilter. One of the mechanical aeration types used to provide DO is a bubble aerator. A bubble aerator with a finer size leads to a higher interfacial area and induces higher DO transfer [15,16]. As a result, the TAN removal efficiency of an MBBR with a similar reactor utilizing a fine bubble aerator was higher (45%) compared to a larger or coarse bubble size (33%) [17,18].

A study was done to review the properties of microbubbles and size measurement from available bubble generation technologies and provides the perspective of future major applications in water and wastewater treatment [19]. Another review focuses on applying Micro–Nano-Bubble (MNBs) generators for domestic and industrial wastewater treatment [20]. The MNBs technology considers an effective method to improve the adhesion of suspended particles due to the unique characteristics of bubbles, such as small-sized bubbles, higher surface area, slow rising velocity, negatively charged zeta potential, generation of free radicals, and stability. The MBBR applies through conventional nitrification and simultaneous nitrification–denitrification pathways for residual water of the RAS [21]. However, there is no study on the effect of the bubble size and oxygen volumetric transfer on the biofilm growth and microbial communities concerning TAN removal efficiency in treating RAS residual water. Therefore, the objective of this review is to provide an updated evaluation of bubble size and oxygen volumetric transfer of the aerator on TAN removal efficiency and the effect of bubble size on the growth and microbial communities of biofilms in biofilters applied for the treatment of residual water from an RAS.

## 2. Materials and Methods

This review aims to understand the effect of bubble aeration on ammonia removal efficiency and biofilm growth in biofilters applied in RASs. A systematic review with four steps was conducted to achieve this goal. The first step was identifying the database and then screening the result from the title and abstract. Furthermore, the selected papers in

the full text were analyzed. The last step was choosing a group of documents to include. In this review, the PRISMA guideline was also adopted.

### 2.1. Objective

The main objective of this study was summarized in two research questions (RQ).

RQ1: How does bubble size affect oxygen transfer and ammonia removal efficiency in various types of biofilters in RASs?

RQ2: What is the relation between aeration and biofilm growth to remove ammonia in various types of biofilters in RASs?

Several keywords were determined from the research questions. The keywords, which consist of bubbles (and synonyms such as nanobubble), aeration, ammonia, biofilter (and correlated expressions such as MBBR), biofilm, and RAS, were included in the screening process. The Boolean operators were combined with these keywords and used as a search expression [22]. The search was carried out in ScienceDirect and Google Scholar. From the search, 1899 documents were found, as shown in Table 1, and proceeded to the screening step.

**Table 1.** Identification step results.

Search Local	Search Expression	Search Result	Types of Documents
ScienceDirect	(bubble! OR nanobubble!) AND (aeration) AND (ammonia) AND (biofilter! OR MBBR!) AND (biofilm!)	445	<ul style="list-style-type: none"> <li>• 55 Review articles</li> <li>• 239 Research articles</li> <li>• 19 Encyclopedia</li> <li>• 79 Book Chapters</li> <li>• 10 Conference abstracts</li> <li>• 2 News</li> <li>• 3 Short communication</li> <li>• 38 Other</li> </ul>
Google Scholar	(bubble! OR nanobubble!) AND (aeration) AND (ammonia) AND (biofilter! OR MBBR!) AND (biofilm!) AND (RAS!)	454	<ul style="list-style-type: none"> <li>• 27 Patents</li> <li>• 43 Review articles</li> </ul>

### 2.2. Screening

This step determined the year of publication screening from the total identified documents. The years of publication were limited to 2011–2022 in ScienceDirect and 2011–2021 for Google Scholar. As a result, 324 documents from ScienceDirect and 320 documents from Google Scholar were selected. Then, the type of paper screening was utilized to exclude all documents except for research papers. When the filtering considered only “research article” in ScienceDirect, 170 articles were received.

In contrast, in Google Scholar, the received articles totaled 251. Then, screening was performed by checking the title and abstract. If the title and abstract contained one or more keywords or search queries, it was included for full-text analysis. Consequently, 369 articles were excluded by this step. Furthermore, the screening step was done in November–December 2021.

### 2.3. Eligibility

Eligibility assessment was started by downloading the 52 articles from 2 search engines. Then, the 52 articles were analyzed, seeking the effect of bubble aeration on reducing ammonia nitrogen and its effect on the biofilm growth of biofilters. Out of 52 articles, five were excluded due to duplication, and 28 were excluded because the aeration/biofilter was not implemented in an RAS.

## 2.4. Inclusion

After full-text analysis, 19 articles were included in this study. These articles described the effect of bubble aeration on biofilm growth and reduced ammonia in the biofilter at the lab or a pilot of an RAS. The articles searched were published in the time range between 2011 and 2022. The analysis steps introduced in the PRISMA procedure are shown in Figure 1.

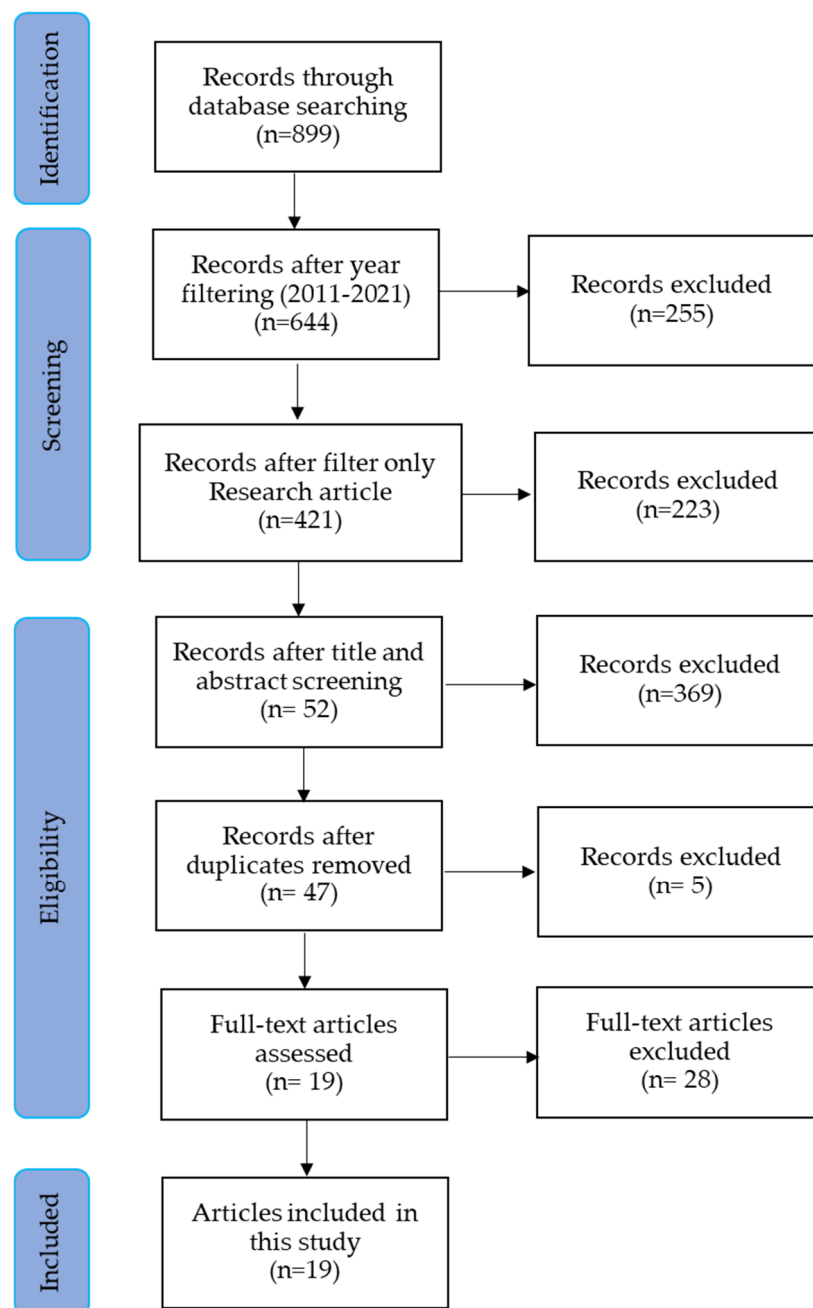
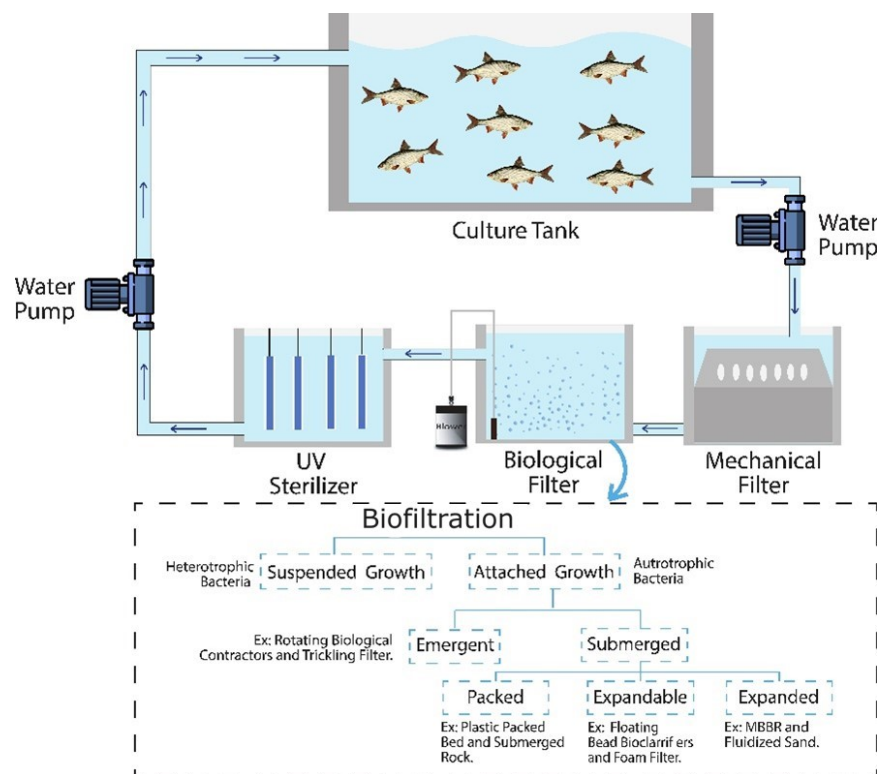


Figure 1. Document selection based on PRISMA workflow.

## 3. Types of Biofilter in RASs and Role of Bubble Aeration in Biofilter

There are two well-known biofiltration types based on the growth of microorganisms, i.e., attached and suspended growth, as shown in Figure 2. A fixed or attached film system is generally used in the RAS since it is more stable than a suspended growth system. The fixed film is classified as the emergent filter or the submerged filter. The emergent filter uses a water cascade that directly flows over biofilter media to maximize oxygen transfer [7].

The trickling filter is one emergent filter that uses wastewater infiltration sprayed from the top of the filter towards the bottom drain to form a biofilm on the surface of the packing media. Biofilm formation degrades the organic matter in wastewater passing through the packing media [23]. In comparison, the rotating biological contactors treat the wastewater by rotating the media in and out of the wastewater [24].



**Figure 2.** Types of biofilters in RASs.

In the submerged filter, surfaces of submerged biofilter media are used to support the attachment and growth of microbes, subsequently increasing biofilm growth [25]. Three types of submerged filter media are based on dynamic behavior: packed bed, expandable, and expanded. The packed bed filter utilizes a compact and immobile stack of media that behaves as porous media [26]. This biofilter creates a biofilm that is more stable and is not easily damaged in a small amount of oxygen [27]. The expandable filter utilizes bead media simultaneously to stimulate the growth of desirable microbes and to remove waste from the water [28]. The filtration process occurs by capturing suspended solids of the recirculating wastewater that passes through the packed beads media and subsequently causes pollutant degradation [29]. Thus, periodic cleaning of the packed beads is necessary to maintain the filtration performance and is achieved by mechanical, pneumatic, or hydraulic means [28,30]. In contrast, the expanded filter of an MBBR utilizes the motion of media; in this condition, the cyclic formation and erosion of biofilm occurs because of the hydraulic and pneumatic behavior of media [7]. However, an efficient biofilm for the MBBR needs a high specific surface area and to be provided a large growth zone. Therefore, precaution is needed to control the hydrodynamic behavior of aeration.

Bubble aeration is critical in determining biofilter efficiency in reducing ammonia nitrogen, as described in Figure 3. Bubble aeration utilizes air or gas in the form of bubbles to provide dissolved oxygen to the media of biofilm growth. The rising gas bubbles transfer oxygen into the liquid phase as dissolved oxygen. The dissolved oxygen is diffused into the biofilm towards the oxidative-phosphorylation sites. The biofilm is attached to the media as a solid phase. The oxygen transport suffers various resistances from the bubbles, liquid, and solid phases, as seen in Figure 3e. The resistance of the bubble comes from the

liquid film resistance ( $k_L$ ) around the bubble, which usually controls the overall transfer rate from the bubble to the liquid phase and the final destination of the biofilm, as seen in Figure 3e [31].

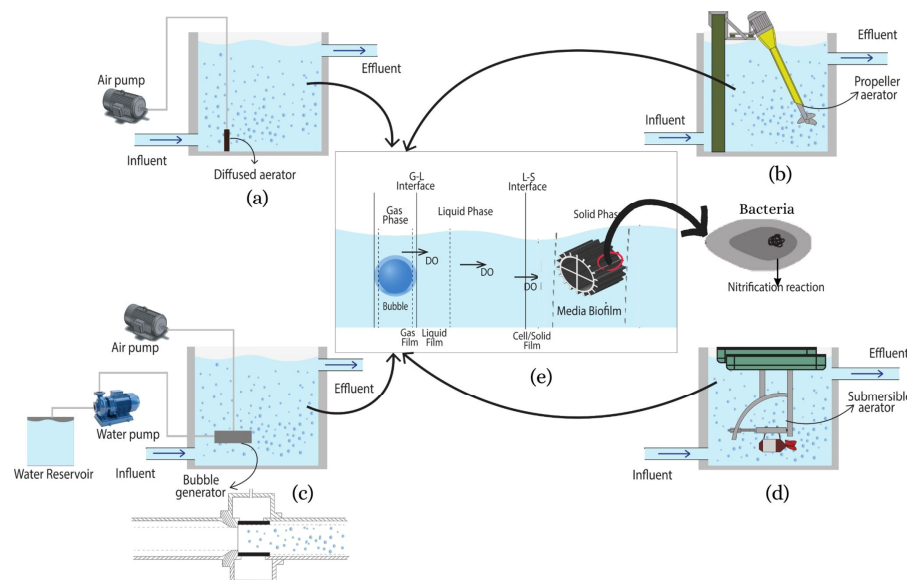


**Figure 3.** Oxygen transfer at various types of bubble aerators (a) diffused aerator; (b) propeller aerator; (c) bubble generator; (d) submersible aerator, and (e) transfer oxygen process in the biofilter.

Bubble aerators are classified as a diffused, propeller, and submersible, as shown in Figure 3a–d. The characteristics of generated bubbles depends on the mechanism of bubble formation, the location, and the interaction of the generator with water. For example, pressurized air or oxygen gas from a blower or compressor introduced in the diffuser method generated bubbles with the size and distribution of the bubbles depending on the pore size and morphology of the diffuser [32]. In comparison, the high-velocity agitated propeller-generated bubbles create highly dynamic behavior causing turbulence in the water, and the bubbles mix easily with the water. The submersible aerator consists of a pump that draws atmospheric air through a hollow suction pipe connected to the propeller at the other end submerged in water. The propeller rotates at a high-speed rpm, enough to cause air suction in the hollow pipe to generate bubbles due to the turbulent water and air mixture created by the propeller [33].

In contrast, the Bernoulli principle of fluid mechanics generates smaller and uniformly distributed bubble sizes, where the free air enters the pipes due to pressure differences in the pipes and the atmosphere [34]. In this review, the application of diffused aerators and bubble generators is highlighted in terms of their bubble size and oxygen transfer concerning the biofilm growth or biofiltration performances.

### 3.1. Bubble Size

Many researchers classified bubbles as nanobubbles (diameter  $<200$  nm), fine bubbles (diameter  $200\text{--}10\text{ }\mu\text{m}$ ), microbubbles (diameter  $\leq 50\text{ }\mu\text{m}$ ), and macro bubbles (diameter  $2\text{--}5\text{ mm}$ ) [35,36]. However, ISO 20480-1 classifies a bubble with a volume equivalent to diameter. Thus, bubble terms based on their size are defined as micro, fine, and ultrafine bubbles/nanobubbles ranging from  $1$  to  $100\text{ }\mu\text{m}$ , less than  $100\text{ }\mu\text{m}$ , and less than  $1\text{ }\mu\text{m}$ , respectively [37]. In conventional aerators, there are medium bubbles with a diameter of  $1.5$  to  $3\text{ mm}$ , and giant bubbles or coarse bubbles with a diameter of over  $3\text{ mm}$ .

Fine bubbles can be generated from a porous diffuser or membrane with tiny holes, while medium bubbles from an orifice, and coarse bubbles through pipes or plates [38]. The



relation between the bubble size ( $d_b$ ) and pore size ( $d_o$ ) can be written in Equation (1), where  $g$  is gravitational acceleration,  $\rho$  is the density of the liquid, and  $\sigma$  is surface tension [39].

$$\frac{d_b}{d_o} = 1.8 \left[ \frac{\sigma}{\rho g d_o^2} \right]^{1/3} \quad (1)$$

### 3.2. Biofilm Growth

Biofilms are groups of microbial cells attached to a solid surface or a media and encased with a matrix. The matrix contains microbial biopolymers composed of extracellular DNA, exopolysaccharides, and proteins [40]. Figure 4 shows the growth phase of the biofilm from the attachment stage to the release stage and its correlation with bubble size. The smaller size of the bubble, the more the microbial community is increased. The first stage of biofilm growth is reversible attachment. In this stage, free-floating (planktonic) bacteria begin to adhere to media acting as biocarrier surfaces. However, the bacteria are not fully attached and are possibly separated from the formation before being wholly attached. The second stage is irreversible bacteria binding. Bacteria begin to adhere perfectly and grow into mature biofilms due to the presence of an extracellular polymeric substance (EPS). The production of a slime-like layer from the EPS supports the structure of the biofilm. EPS is composed of proteins, polysaccharides, and nucleic acids. Then in the third stage, or the maturation stage, bacteria have a complex architecture, pores, and charges far from the substrate. At this stage, there is more protein, consequently increasing the bacterial number and diversity of the biofilm. When smaller bubbles are applied, more efficient oxygen transfer is generated to create more protein to promote an enhanced number and diversity of bacteria. In the fourth stage, strong bacterial adherence occurs due to matured biofilm formation. The last stage is detachment, where bacteria are detached from the biofilm due to the reduction of the EPS or lack food supply [41,42]. Biofilm growth rate ( $\mu$  in  $\text{h}^{-1}$ ) is calculated using Equation (2) where  $X_2$  ( $\text{mg}/\text{cm}^3$ ) is the density of biomass at the end of the experiment,  $X_1$  ( $\text{mg}/\text{cm}^3$ ) is the density of biomass at the first period of the experiment, and  $\theta$  (h) is the experiment period [43].

$$\mu = \frac{(X_2 - X_1)}{X_1 \times \theta} \quad (2)$$

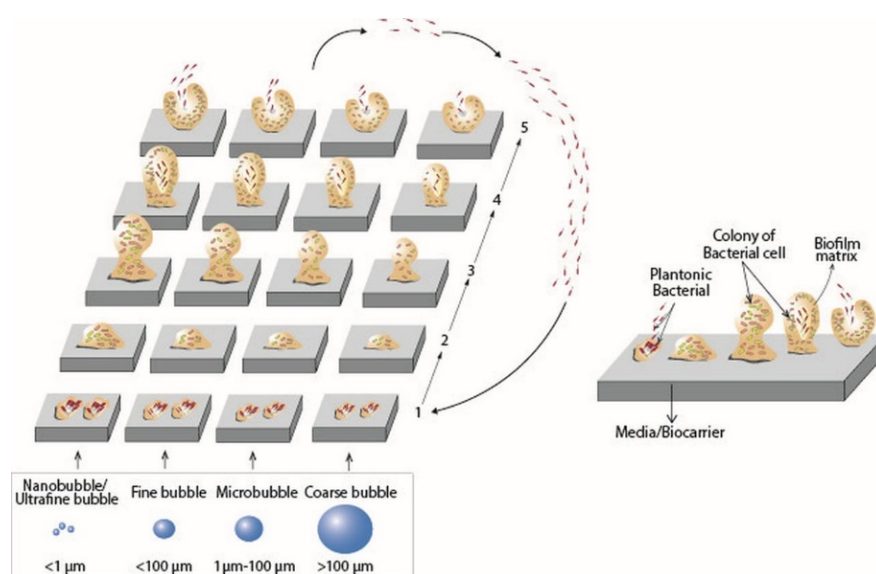
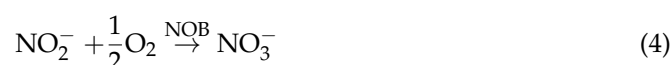
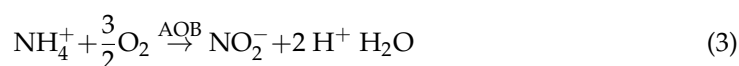


**Figure 4.** Effect of bubble size on the phase of biofilm growth: (1) Adhesion stage, (2) Extracellular Polymeric Substance (EPS) production, maturation stage, (3) formation of complex structure, (4) strong-adherence bacterial stage, and (5) cell detachment from the biofilm.

### 3.3. Nitrification in Biofilm

Characteristics of bubbles affect the oxygen transfer efficiency from gas through water into the biofilm [44]. Efficient oxygen transfer ensures sufficient DO for the nitrification process inside the biofilm. Nitrification is extremely important in reducing harmful ammonia in the RAS. Nitrification is one of the biological processes where  $\text{NH}_3$  and  $\text{NH}_4^+$  are oxidized to nitrate in two steps with the help of nitrifying bacteria with a reaction, as seen in Equations (3) and (4) [45]. Ammonium oxidizing bacteria (AOB) such as *Nitrosomonas* and *comammox* are responsible for converting ammonium nitrogen into nitrite ( $\text{NO}_2^-$ ). Then, nitrite is converted into nitrate with the help of nitrite-oxidizing bacteria (NOB) such as *Nitrospira* and *Nitrobacter*.



### 3.4. Oxygen Transfer

An effective nitrification process depends on having enough dissolved oxygen obtained from the aerator with a small bubble size. Bubbles with smaller sizes have higher oxygen mass transfer [15]. Furthermore, small bubbles facilitate oxygen distribution through biofilm for the nitrification process. Thus, a smaller bubble size potentially produces higher ammonia degradation than a coarse bubble size. The relation between bubble size and oxygen transfer can be associated with specific interfacial area  $a$ . This value is related to fractional gas hold up  $\varepsilon_g$  and Sauter mean diameter of bubble  $d_b$  as written in Equation (5) [16,46]. Based on this equation, a smaller bubble diameter increases the gas–liquid interfacial area.

$$a = \frac{6\varepsilon_g}{d_b(1 - \varepsilon_g)} \quad (5)$$

The value of  $a$  influences the mass transfer rate, which can be described with  $dC/dt$  as written in Equation (6) [47] where  $dC$  is the change of oxygen concentration with time  $dt$ ,  $k_L a_{(T)}$  is the oxygen volumetric transfer coefficient at temperature  $T$  (the temperature at the time of the experiment), which is determined from  $K_L$  (liquid film coefficient) and  $a_{(T)}$  (unit interfacial media at a certain temperature),  $C^*$  is the oxygen saturation, and  $C$  is the DO concentration at time  $t$ . The  $k_L a_{(T)}(C^* - C)$  is the Oxygen Transfer Rate (OTR). The value of  $k_L a_{(T)}$  is an indicator of DO mass transfer in biofilters which is one of the critical factors in the aeration rate [14,48]. Furthermore,  $k_L a_{(T)}$  is calculated using Equation (7), which can be integrated from Equation (6) [49].

$$dCdt = k_L a_{(T)}(C^* - C) \quad (6)$$

$$\ln \left( 1 - \frac{C}{C^*} \right) = k_L a_{(T)} t \quad (7)$$

## 4. Results and Discussion

### 4.1. Biofilm Performance with Bubble Aeration

#### 4.1.1. Effect of Medium and Coarse Bubble Aeration on the Biofilter Performance

The recent development of bubble aeration applied for fixed film biofilters is summarized in Table 2. The larger size of bubble aeration affected the media in the MBBR to maintain biofilm thickness by shear forces and allow diffusion transport of DO and ammonia ions to the biofilm. However, aggressive aeration on the media caused excessive biofilm erosion [50]. Medium bubble aeration was used to aerate five types of media with different surface areas and percentages of voidage in a pilot plant MBBR. The surface area of various media with spherical shapes, such as media 1 (Biofil), 2 (Bioball), and 3 (Biomarble),



were 135, 220, and 310 m<sup>2</sup>/m<sup>3</sup> with voidage of 95, 92, and 90%, respectively. In contrast, the surface area of media 4 (Biopipe) and 5 (Biotube) with cylindrical shapes were 600 and 1000 m<sup>2</sup>/m<sup>3</sup> with voidage of 82.5 and 80%, respectively. The airflow rate was controlled at 3.6–18.7 m<sup>3</sup>/m<sup>2</sup>.h to keep stable DO levels. The ammonia removal efficiencies have reached 50 ± 13%, 64 ± 13%, and 63 ± 7% for media 1, 2, and 3, respectively after 30, 22, and 17 days. Media 4 and 5 have achieved ammonia removal efficiency percentages of, respectively, 32 ± 17% after 46 days and 34 ± 5% after 47 days. The highest removal efficiency has been achieved by media 2 due to the open spherical structure, higher voidage compared to media 3, 4, and 5, and even higher surface area than media 1. These factors caused an increase in oxygen distribution all over the media, and they offered larger surface areas for biofilm to attach to the media surface [17].

A coarse bubble from a disc diffuser was tested in the MBBR to enhance the media movement and degassing. Three media (MB3, K1 Kaldness, AMB) were used as MBBR media for water treatment in the red drum fingerlings hatchery. The highest TAN removal efficiency for those three media was generated when the DO was 6.9 ± 0.7 mg/L in high feed load rates (8.2 kg feed/m<sup>3</sup> media). The TAN removal efficiency reached 15.6 ± 0.4%, 15.4 ± 0.2%, and 11.6 ± 0.3% for MB3, K1 Kaldness, and AMB, respectively. MB3 media resulted in the highest TAN removal efficiency because it had a larger surface area (604 m<sup>2</sup>/m<sup>3</sup> surface area) than the other media. The firm structure and larger size of MB3 media were easily aerated and provided enhanced TAN removal rates [50].

Meanwhile, coarse bubble diffusers were also tested on a lab-scale MBBR by maintaining DO concentration at 5.5–7.5 ± 0.5 mg/L [51]. The novel sponge carrier (SB) and Kaldness K5 were used as biofilm media. The TAN removal efficiency of SB media was 91.65 ± 1.3% which was higher than Kaldness media (86.67 ± 2.4%) for 6 h of hydraulic retention time (HRT). Higher removal efficiency in SB media was due to the enhancement of aerobic conditions, which led to a complete nitrification process. In addition, the porous structure of the SB media provided sufficient protection, so the bacteria were not easy to wash away [51].

Another study compared a coarse bubble diffuser and biofilm chip media (900 m<sup>2</sup>/m<sup>3</sup> surface area) to control the water quality in an RAS for Atlantic Salmon smolt. The system consisted of three MBBRs with three nominal alkalinity treatments: 10 mg/L, 70 mg/L, and 200 mg/L. The DO was controlled between 85% and 90% of saturation in the experiment. The TAN concentration of inlet MBBR based on the 10 mg/L, 70 mg/L, and 200 mg/L alkalinity treatments were 0.65 ± 0.08, 0.43 ± 0.04, and 0.39 ± 0.05 mg/L, respectively. While the TAN generated from the outlet of MBBR based on the 10 mg/L, 70 mg/L, and 200 mg/L alkalinity treatments were 0.39 ± 0.06, 0.22 ± 0.03, and 0.23 ± 0.04 mg/L, respectively. The 70 mg/L alkalinity treatment contributed the highest mean TAN removal efficiency (around 50%) in the 20 week experiment. This efficiency occurred due to the higher inlet TAN of the 10 mg/L alkalinity treatment causing higher removal rates based on kinetic studies [52]. Similarly, a coarse bubble diffuser with a high flow rate (3.17 L/min) was applied to enhance the media movement of K1 Kaldness (500 m<sup>2</sup>/m<sup>3</sup> surface area) in an MBBR for rearing Florida Pompano. The DO concentration was 8.2 ± 1.0 mg/L in the culture tanks. During the experiment, the average TAN concentration was 0.46 ± 0.27 mg/L, and TAN removal per pass was 33.0 ± 11.9% with a range of 8.3–62.4% [53]. At the same time, a coarse bubble was applied as the aeration system to ensure oxygen saturation of >100% for the MBBR in RAS culturing of European sea bass (*Dicentrarchus labrax*). Sea bass culture was exposed to four different nitrates: control (C) 0 mg/L, low nitrate (LN) 125 mg/L, medium nitrate (MN) 250 mg/L, and high nitrate (HN) 500 mg/L. Mean values (±SD) of TAN for different nitrate C, LN, MN, and HN had reached 0.10 ± 0.09 mg/L, 0.11 ± 0.10 mg/L, 0.11 ± 0.08 mg/L, and 0.11 ± 0.08 mg/L, respectively [54]. The MBBR with coarse bubbles showed that the TAN concentration meets the safety range for culturing sea bass (<2–6 mg/L) [55,56].

**Table 2.** Summary of biofilter performance at various types of aerator and biofilter types in RASs.

Type of Aerator	Biofilter Type (Volume in L)	RAS Culture Species	Media Type (Surface Area in m <sup>2</sup> /m <sup>3</sup> )	DO (mg/L)	$k_L a_{(T)} t$	Performance Ammonia Removal (%)	Ammonia Concentration (mg/L)	Reference
Medium bubble diffuser	MBBR (2000)	N/A	Bioball (220)	6.1 ± 0.9	N/A	64 ± 13	N/A	[17]
Coarse Diffuser	MBBR (6360)	Red drum fingerlings ( <i>Sciaenops ocellatus</i> )	MB3 (604)	9.9 ± 1.9	N/A	15.6 ± 0.4	1.055	[50]
Coarse bubble diffuser	MBBR (5.5)	Not specified	Novel sponge biocarrier (N/A)	5.5–7.5 ± 0.5	N/A	91.65 ± 2.4	0.83 ± 0.31	[51]
Coarse bubble diffuser	MBBR (7000)	Atlantic salmon parr ( <i>Salmo salar</i> )	N/A	7.3	1.89	50 ± 3	0.22 ± 0.03	[52]
Coarse Bubble diffuser	MBBR (410)	Florida pompano ( <i>Trachinotus carolinus</i> )	K1 Kaldness (N/A)	8.2 ± 1.0	1.39	62.4	0.46 ± 0.27	[53]
Coarse bubble diffuser	MBBR (N/A)	European sea bass ( <i>Dicentrarchus labrax</i> )	N/A	10 ± 0.9	N/A	N/A	0.11 ± 0.08	[54]
Coarse bubble diffuser	Membrane Filter (N/A)	N/A	Commercial mixed-cellulose (MC) membranes (N/A)	6.75	1.54	38	7.81	[12]
Microbubble diffuser	airlift fluidized bed reactor (115)	Nile Tilapia ( <i>Oreochromis niloticus</i> )	Granular activated carbon (N/A)	4.16	N/A	27	0.104	[2]
Fine bubble diffuser	BAF (1.6)	N/A	Puzzolane material (1740)	>2.1	0.31	50–80	N/A	[57]
Fine bubble diffuser	Fixed bed reactor (3.5)	N/A	Polycaprolactone 114 (PCL) (N/A)	5.63 ± 0.57	1.73	57.14	1.93 ± 0.37	[58]
Nanobubble generator and combination with coarse bubble diffuser	BAF (4.75)	N/A	Volcanic rock filter (N/A)	6.52	2.06	98.02	N/A	[59]
Nanobubbles generator	Membrane Filter (N/A)	N/A	Commercial mixed-cellulose (MC) membranes (N/A)	8.55	1.92	75	3.15	[12]

#### 4.1.2. Effect of Micro, Fine, and Nanobubble Aeration on the Biofilter Performance

Recently, aeration systems with a finer bubble for RASs have gained much interest because of their high mass transfer and long-term existence in an aqueous environment. The RAS with cultured Nile Tilapia used microbubble aeration aimed to maintain the correct concentration of DO. This RAS used the aeration system of the airlift fluidized bed reactor. By maintaining the air flow rate at 10 L/min, the aerator guaranteed the needed quantity of DO concentration (4.61 mg/L). Thus, the mean removal efficiencies of BOD, COD, phosphorous, TAN, and total nitrogen had reached 47, 77, 38, 27, and 24%, respectively [2].

A fine bubble diffuser generating micro- and nanobubble was evaluated for the aeration performance in a BAF reactor intended to reduce the concentration of ammonia nitrogen. The DO concentration was maintained  $>2$  mg/L, and the aeration rate was kept at 0.33 L/min. The sampling points were made in some places based on the biofilter's depth, 3, 4.5, 7.5, 12.5, 22.5, 32.5, and 40 cm. This investigation aimed to know the effect of hydraulic retention time (HRT) in correlation to biofilter performance. The average DO concentrations in the long term decreased along with biofilter depth. Ammonia removal efficiency between 50% and 80% received from sections between 3–7.5 cm depth was associated with high availability of DO (over 2.1 mg/L), and formed higher biofilm thickness (0.4–0.6 mm) [57]. The ammonia concentration was higher at a higher depth (12.5–40 cm). Higher ammonia concentrations occurred due to the effect of lower HRT causing high DO demand and consequently lowering the biofilm thickness because of a decrease in the availability of DO compared to the depth of 3–7.5 cm.

Similarly, a fine bubble diffuser was also used to study the effect of aeration in a fixed-bed reactor [58]. The study consisted of three treatment groups: anoxic, low DO, and aeration, producing DO concentrations ranging from 0.12 to 0.55 mg/L, 1.82 to 3.99 mg/L, and 5.29 to 6.56 mg/L, respectively. All treatments gave a DO concentration below 0.02 mg/L in the outlet. Reduced DO indicated oxygen consumption due to bacterial growth under aerobic conditions. The removal efficiency of  $\text{NO}_3\text{-N}$  after the start-up period of 11–18 days was maintained at 90% in the anoxic and low DO treatments. However, it decreased to 75% for the aeration treatment at the end of the experiment. Although aeration treatment showed a low  $\text{NO}_3\text{-N}$  removal efficiency, Total Nitrogen (TN) removal efficiency was the highest (90%) among other treatments. This efficiency in TAN removal was possibly due to complete nitrate removal, designating the effective nitrate transformation into nitrogen gas. Conversely, in the anoxic and low DO treatments,  $\text{NO}_3\text{-N}$  might be transformed into ammonia or nitrite ( $\text{NO}_2$ ), and they remained in the system. In addition, the average TAN accumulation in all three treatments was observed at  $1.93 \pm 0.37$ ,  $1.37 \pm 0.15$ , and  $1.72 \pm 0.46$  mg/L during the steady-state period [58]. Therefore, the aeration efficiency in aerobic systems enhanced the total removal efficiency, especially in removing nitrite.

An aerator made from a combination of nanobubbles (420 nm) and air bubbles (coarse bubbles) has also been tried and compared to just nanobubbles used for biologically aerated filters (BAF) in a laboratory-scale wastewater treatment plant (WWTP) [59]. Both treatments used the same filter size and eight variations of aeration treatment with different oxygen resources (air/water ratio). The application of only nanobubbles enabled obtaining  $\text{NH}_4^+ - \text{N}$  and TN removal efficiency at the maximum levels of 74.89 and 70.69%, respectively, if the DO concentration was 5.59 mg/L. When the combination of nanobubbles and coarse bubbles was used in BAF, the highest  $\text{NH}_4^+ - \text{N}$  and TN removal efficiency were obtained at 98.02 and 54.98%, respectively, if the DO concentration was 6.52 mg/L. The DO was obtained at 6.52 mg/L when the air/water ratios were set up to be 0.2 and 0.5 for nanobubble and coarse bubbles, respectively. The highest removal efficiency of  $\text{NH}_4^+ - \text{N}$  and TN were due to the dynamic interaction between the bubbles and media and the roles of bubbles size in oxygen mass transfer efficiency from bubbles to media at a particular air/water ratio. In addition, the coarse bubbles played an essential role in reinforcing the shear stress to the biofilm in correlation to the cyclic growth of biofilm formation. In contrast, nanobubbles gave effective mass transfer to provide high dissolved

oxygen in the media. The allowable shear stress of the coarse bubble on the biofilm enabled film detachment. In addition, it maintained the thickness to effectively transport nutrients and oxygen into the biofilm [59]. Thus, higher dissolved oxygen generated in nanobubble aeration could provide higher TAN removal than coarse bubble aeration systems.

In contrast, nanobubbles with an aeration rate of 0.2 L/min was used in the lab-scale experiment, and coarse bubble aeration was applied to the system as a comparison [12]. A membrane filter of 1.2 µm thickness (ø =50 mm) commercial mixed-cellulose (MC) membrane was used as the biofilm carrier. The higher DO peak (10.012 mg/L) in biofilm has resulted in using nanobubble aeration compared with coarse bubble aeration (8.581 mg/L). The dissolved oxygen generated from nanobubble aeration remained higher than the coarse bubbles after 200 s. Consequently, higher ammonia removal (75%) has been achieved using nanobubble aeration. Thus, it also remarked that higher transfer oxygen in nanobubble than coarse bubble was considered responsible for the higher removal efficiency [12].

#### 4.2. Biofilm Growth

##### 4.2.1. Microbial Community

In wastewater treatment, the microbial community is an essential factor affecting biofilter performance to reduce ammonia through nitrification. One way to determine biofilm diversity is using the Shannon diversity index [60]. The Shannon index was used to describe variation at multiple levels of genetic organization from single nucleotide polymorphisms (SNP) through whole species or larger taxonomic units to ecosystems [61]. The Shannon index was calculated from the operational taxonomic unit (OTU). The OTU is a collection of 16S rRNA sequences with specific sequence divergence percentages [62]. We can know the number of necessary bacteria such as AOB and NOB in biofilm from the OTU. The diversity in the biofilm, which correlated with the bubble aeration, is summarized in Table 3.

**Table 3.** Summary of microbial community in biofilter.

Aeration Type	Biofilter Type (Volume in L)	Biofilter Volume (L)	Culture Species	Shanon	Performance		Reference
					Ammonia Removal (%)	TN Removal (%)	
Coarse bubble diffuser	MBBR	0.7	N/A	1.30	97.1	N/A	[63]
Coarse bubble diffuser	MBBR	N/A	Atlantic salmon post-smolts	2.87	50	N/A	[64]
Coarse bubble diffuser	BAF	10,850	Seawater RAS	5.04	41.7	41.3	[65]
Coarse bubble diffuser	BAF	10,850	Seawater RAS	8.36	85	N/A	[66]
Coarse bubble diffuser	MBBR	5	N/A	2.30	96	N/A	[13]
Coarse bubble diffuser	MBBR	0.4	N/A	2.85	36.04	N/A	[11]
Fine bubble diffuser	MBBR	0.4	N/A	2.88	51	N/A	[11]

Coarse bubble aeration was applied to investigate microbial communities in three MBBRs with different salinity [63]. The system used an air stone aerator to keep oxygen concentration at  $7.2\text{--}7.6\text{ mg O}_2\text{ L}^{-1}$  in three MBBRs with K1 AnoxKaldness media. Each MBBR was fed with basal synthetic wastewater medium (freshwater reactor or FR), a mix of tap water and seawater (brackish reactor or BR), or only seawater (seawater reactor or SR). Nitrifying bacteria were classified in the family of *Nitrosomonadaceae* (AOB) with a composition of  $6 \pm 0.4\%$ ,  $34.7 \pm 1.9\%$ , and  $14.7 \pm 2.3\%$  for FR, BR, and SR, respectively. NOB consisted of *Nitrospiraceae*, *Nitrospira*, and *Nitrobacter*. The OTU of NOB was  $27 \pm 1.0\%$ ,  $8.1 \pm 1.3\%$ , and  $13.4 \pm 1.7\%$  for FR, BR, and SR, respectively. The average ammonia removal efficiency of FR, BR, and SR reached 97.1%, 95%, and 95.4%, respectively. The other nitrification performances of the three reactors might be related to the ratio of NOB and AOB. The higher ammonia removal efficiency was attained from FR because of a higher population of NOB than AOB (NOB:AOB ratio of 4:1). The dominance of NOB over AOB correlated with good nitrification. Nevertheless, FR resulted in a lower Shannon diversity value ( $1.3 \pm 0.08$ ) than SR ( $1.4 \pm 0.56$ ) [63]. Similarly to coarse bubbles, this

was also used in another study to investigate microbial communities in the biofilm of the MBBR. Three salinities, 12, 22, and 32 ppt, were used in a semi-commercial RAS for salmon post-smolt treatment. From the study, sampling was done in the MBBR inlet, outlet, and biofilm. Biofilm communities are higher regarding their Bray–Curtis similarities in comparison between time points. Biofilm communities seemed less influenced by salinity than water communities and more stable over time. The nitrifying biofilm was adapted to increase salinity over 2–4 weeks. The highest removal TAN was received when the average Bray–Curtis similarity was 0.75, and the Shannon index was 2.87 [64].

A coarse bubble was used as aeration in an experiment with four different microbial agents (DW, CES-1, BM-S-1, KBM-1) for a marine finfish RAS [65]. This study investigated four bioreactors: packed, aerated, floating, and mesh biofilters. Aeration was provided with a flow rate of 800 L/min in a floating bed biofilter. The ammonia nitrogen degradation rate reached 13.4, 41.0, 33.9, and 41.7% for DW, CES-1, BM-S-1, and KBM-1 over eight days of the experiment. The result showed that on the fourth day of the experiment, the KBM-1 community was more diverse than BMS-1, with 575 OTU and a 5.04 Shannon value. In all treatment groups, *proteobacteria* were dominant in 60–70% at the phylum level. Another abundance in the system consisted of *Bacteroidetes*, *Firmicutes*, *Fusobacteria*, *Actinobacteria*, and others [65]. A similar plant was also used to investigate bacterial diversity in a seawater RAS. The system used a packed bed biofilter, aerated biofilter, floating bed biofilter, mesh biofilter, and maturation tank [66]. Bubble aeration with a flow rate of 1000 L/min was applied as an aeration system in the aerated biofilter. The result of the experiment showed that the packed bed and mesh biofilter contained a high number of nitrifying bacteria. *Phylotypes* related to *Nitrosomonadaceae*, which contained most of the AOB occupied 0.06–3.56% (average 1.22%) of the packed bed biofilter and 1.19–6.41% (average 2.80%) of the mesh biofilter. The *Nitrospirae* group was also detected at values 0.02–10.56% (average 2.55%) and 0.32–9.45% (average 3.57%) in the packed bed and mesh biofilter, respectively. *Nitrospina*, a nitrite-oxidizing group belonging to *Deltaproteobacteria*, was detected up to 9.0%. This result showed that packed bed and mesh biofilter types had affected ammonia removal in the RAS. Whereas in the aerated biofilter, the value of *Nitrosomonadaceae* was about 0.1–1% and *Nitrospirae* about 0.5–1.5%. The highest Shannon Index was 8.36 for the packed bed biofilter [66].

Coarse bubble aeration with a 48 L/min flow rate and three media (microfiber carrier, nanofiber carriers, and AnoxKaldness K3) was used in a lab-scale MBBR [13]. As a result, a relative abundance of nitrifying bacteria, *Nitrosomonas* (AOB) showed more noticeable development between month 1 (0.289%) and month 3 (1.835%) on microfiber, and *Nitrospira* (NOB) on nanofiber (from 3.11% on month 1 to 11.20% on month 3) and AnoxKaldness (from 5.41% on month 1 to 10.22% on month 3). AOB preferred an environment with a high amount of biomass and a large active area; meanwhile, NOB thrives better in slowly forming biofilm. Based on Shannon index diversity, nanofiber obtained the highest number among all media. However, based on respirometry data, the highest O<sub>2</sub> consumption was obtained by microfiber carriers due to the sufficient internal space of the microfiber to allow high-speed capture of biomass. In addition, O<sub>2</sub> consumption in microfiber was increased due to endogenous respiration. Nevertheless, O<sub>2</sub> consumption of nanofiber media increased with time due to the slow increase in biofilm activity. In comparison, AnoxKaldness K3 had a less effective structure because of a longer bacterial colonization time [13].

Other studies reported that fine bubble and coarse bubble aeration were applied in lab-scale experiments to study the influence of aeration on the biofilter microbial community [11]. Three media were used for growing microbial biofilm in a working volume of 0.4 L in a lab-scale batch reactor. The aeration rate was divided into six stages: fine bubble 0.1 L/min (Startup and Stage A), fine bubble 1.0 L/min (Stage B), coarse bubble 1.0 L/min (Stage C and Stage D), and coarse bubble 5.0 L/min (Stage E). In stage A, all biofilms resulted in relatively high abundances of autotrophic AOB/NOB (*Nitrosomonas*  $7.49 \pm 1.89\%$  and *Nitrobacter*  $7.4 \pm 1.89\%$ ). By the end of stage B, all biofilms became



more heterotrophic ( $11 \pm 2.4\%$  *Comamonas*,  $10.3 \pm 3.3\%$  *Ferruginibacter*, and  $4.8 \pm 0.9\%$  *Bradyrhizobium*) and less autotrophic. *Ferruginibacter* may play a role in the produced and exported EPS. A similar pattern occurred in stages C and D ( $3.3 \pm 0.4\%$  *Nitrobacter*). At the end of stage E, the biomass detachment occurred. In stages A until D, ammonia flux increased with increasing aeration. However, it decreased by approximately 50% when coarse bubble aeration was increased in stage E. The decreased ammonia flux was because of the loss of biofilm mass due to the high shear rates. The highest Shannon diversity (2.88) of all media was achieved in stage B. In contrast, in stage E, the Shannon diversity became lower [11].

#### 4.2.2. Biofilm Thickness

Biofilm thickness can influence biofilter oxygen transfer and enhance the microbial community in the biofilter. The biofilm thickness and its influence on reducing TAN are summarized in Table 4. The effect of DO on biofilm thickness was investigated using a coarse bubble in 27.7 L of a cylindrical bioreactor with semi-suspended spindle media [14]. Three phases of aeration were setups in this study, phase I with 1.5 L/min aeration rate (On and Off 30 min) on days 1–5, phase II with 1.5 L/min aeration rate on days 6–56, and phase III with 2.5 L/min aeration rate on days 57–73. Initially, the biofilm thickness was fixed at 10  $\mu\text{m}$ . In the first and second phases, a thin layer of biofilm of no more than 500  $\mu\text{m}$  was formed on the surface of the media. The DO concentration has increased in phase II from 1.95 mg/L to 4.88 mg/L because of the change in aeration mode. In this phase, the thickness of the biofilm grew to 350  $\mu\text{m}$  after 15 days and more than 1000  $\mu\text{m}$  after 25 days. In the third phase, DO increased from 2.21 mg/L to 3.22 mg/L after 55 days, some biofilm detached from biocarrier, and the remained biofilm exhibited lots of pores and channels. Nevertheless, DO was still increased even when the biofilm was very thin, and the maximum depth of DO that could penetrate the biofilm was no more than 900  $\mu\text{m}$ . Total nitrogen removal constantly increased, with max TN removal around 14.3% on the 55th day. However, it decreased slowly after day 55th. This pattern coincided with the growing trend of biofilm [14].

**Table 4.** Summary of biofilm thickness in the biofilter.

Aeration Type	Biofilter Type (Volume in L)	Biofilter Volume (L)	Culture Species	Biofilm Thickness ( $\mu\text{m}$ )	Performance		Reference
					Ammonia Removal (%)	TN Removal (%)	
Coarse bubble diffuser	MBBR	27.7	N/A	1000	N/A	$\pm 14.3$	[14]
Coarse bubble diffuser	MABR	1050	N/A	1000	N/A	$>70$	[67]
Coarse bubble diffuser	Membrane Filter	N/A	N/A	$1016 \pm 236$	38	N/A	[12]
Medium bubble diffuser	MBBR	2000	<i>Litopenaeus vannamei</i>	$71 \pm 22$	$64 \pm 13$	N/A	[17]
Fine bubble diffuser	BAF	1.6	N/A	$470 \pm 50$	50–80	N/A	[57]
Nanobubble generator	Membrane Filter	N/A	N/A	$1188 \pm 322$	75	N/A	[12]
Nanobubble generator and combination with coarse bubble diffuser	BAF	19	N/A	136.1	89.22	34.51	[59]

A coarse bubble was also used in a membrane-aerated biofilm reactor (MABR) to study the impact of oxygen surface loading on biofilm thickness [64]. Approximately  $0.04 \text{ m}^3$  gas volume was applied for aeration and supporting biofilm growth through the gas-permeable membrane. The highest TN removal efficiency in oxygen surface loading of 2.72 was  $>70\%$  at steady state biofilm thickness of 1000  $\mu\text{m}$ . Increased biofilm thickness results in increased total nitrogen removal [64]. Medium bubble aeration with  $3.6\text{--}18.7 \text{ m}^3/\text{m}^2\cdot\text{h}$  flow rate was utilized in the MBBR with five different media [17]. A medium spherical shape media with an initial biofilm thickness of  $71 \pm 22 \text{ }\mu\text{m}$  was evaluated for ammonia removal at various



growth times 30, 22, 17, 46, and 47 days. Approximately 68% of the media's total area ( $148 \text{ m}^2/\text{m}^3$ ) was covered by biofilm. Even though the medium spherical shape owns the open structure lower protected surface area, the circulation and oxygen distribution were preferable in all areas of the media. Consequently, the highest TAN removal efficiency was given to using medium spherical shape media [17].

In comparison, a fine bubble diffuser was evaluated as an aeration system in BAF with different depths of sampling points (3, 4.5, 7.5, 12.5, 22.5, 32.5, and 40 cm) [57]. In three sampling points, the biofilm thickness during steady-state conditions had reached  $0.47 \pm 0.05 \text{ mm}$  (depth of 4.5 cm),  $0.28 \pm 0.05 \text{ mm}$  (depth of 7.5 cm), and  $0.02 \pm 0.01 \text{ mm}$  (depth of 22.5 cm). The thicker biofilm has resulted in a closer position to the aeration source. Higher DO and biofilm thickness in sampling points at a depth of 4.5 cm and 7.5 cm had related to higher ammonia removal [57].

In the lab scale test, biofilm thickness grew faster with nanobubble aeration compared with coarse bubble aeration [12]. The maximum biofilm thickness of  $1188 \pm 322 \text{ }\mu\text{m}$  was obtained using nanobubble aeration within 15 days of the experiment. Nevertheless, the maximum biofilm thickness of  $1016 \pm 236 \text{ }\mu\text{m}$  had produced using coarse bubble aeration. The average aerobic layer increased, triggering of gain in the growth rate for the nanobubbles application. Moreover, biofilm growth comes from protein (PN) and polysaccharides (PS) which is part of EPS. The maximum PN/PS ratio using nanobubble was 7.46, whereas using coarse bubble was 4.81 [12].

Similarly, in an experiment using nanobubble aeration, biofilm thickness increased from  $50.1 \text{ }\mu\text{m}$  to  $109.5 \text{ }\mu\text{m}$  with a PN/PS ratio of 0.2, then decreased to  $78.5 \text{ }\mu\text{m}$  at the end. In contrast, a biofilm thickness of  $116.7 \text{ }\mu\text{m}$  was formed under coarse bubble with a PN/PS ratio of 1 [59]. When equipped with both coarse and nanobubbles for ratios of 1 and 0.2, a thick biofilm was formed ( $136.1 \text{ }\mu\text{m}$ ). In contrast, the biofilm thickness decreased to approximately  $50 \text{ }\mu\text{m}$  using coarse and nanobubbles at the ratios of 0.5 and 0.2. Biofilm thickness in ratio 0.2 was increased compared to ratio 1 due to the addition of nanobubbles enhancing the biofilm core, which is related to bio-volume [59].

## 5. Author Perspective

A summary of the biofilter performances with bubble aeration is represented in Table 2, the  $k_L a_{(T)} t$  value was calculated based on Equation (7) with DO concentration data from the studies presented in Section 4.1. The  $k_L a_{(T)}$  is useful to determine how efficiently oxygen is transferred from the bubble to the water medium [14]. From Table 2, we can see that high DO does not necessarily result in high ammonia removal efficiency; this is related to the effectiveness of the oxygen getting into the biofilm ( $k_L a_{(T)}$ ). Also from Table 2, the highest  $k_L a_{(T)}$  is achieved using nanobubble aeration. Theoretically, the smaller bubble will produce a higher  $k_L a_{(T)}$  because of the larger interfacial area of the bubble [15,16]. Additionally, the high value of  $k_L a_{(T)}$  will produce higher TAN removal efficiency, because the higher value of oxygen is transferred to the cell for nitrification. However, a high ammonia removal efficiency is achieved using coarse bubbles [51] due to the effective contribution of porous media as biofilm media. It showed that the type of media is an important aspect affecting the distribution of oxygen into the biofilm. The  $k_L a_{(T)}$  is not the only factor determining the distribution of oxygen into the film, but also other factors such as microorganism concentration and morphology, medium composition, biocatalyst properties, and also mechanical design, operating conditions, and aeration rate affect the oxygen supply [68].

The other factor contributing to ammonia removal in biofilters is the microbial community of the biofilm. In Table 3, the Shannon index indicates an increasing number of microbial communities in the biofilm. The higher the Shannon index value, the more abundant the microorganisms in the biofilm [69]. Nevertheless, as shown in Table 3, Shannon diversity is not directly correlated with ammonia removal efficiency since this value only represents broad species in the community. Thus, information on the species and numbers of nitrifying bacteria is necessary for their efficiency in ammonia removal.

In addition, the Shannon index was not directly correlated with ammonia removal efficiency, even when conducted in a different type of bubble aeration with a similar reactor [11]. This enhanced efficiency is possible due to the higher number of nitrifying bacteria produced using fine bubble aeration. Additionally, a lower Shannon index can result in high ammonia removal efficiency since it could indicate a high amount of nitrifying bacteria, compared to other studies with a specific ratio of AOB and NOB [63]. In addition, biofilm diversity is affected by some factors such as temperature, pH, ionic strength, and hydrodynamic conditions [70]. Another factor is fluid hydrodynamics that impact oxygen and nutrient transport rates and biofilm cycles [71]. The attachment and detachment of biofilms are stimulated by the hydrodynamic conditions, i.e., air flow rate. A high flow rate can support oxygen and nutrient transport to the surface, contribute to the growth of microorganisms in the microbial layer, and produce the exopolymers that make the attachment stronger. However, the increasing flow rate will raise the shear rates and cause biofilm detachment, yielding a decrease in the amount of biomass attached to the solid surface or media [72]. As long as a higher flow rate is provided, high ammonia removal efficiency can be achieved using coarse bubble aeration [13], but it is more energy-consuming.

The microbial community plays an important role the biofilm growth and thickness. Conversely, biofilm thickness may also affect microbial activity and diversity due to diffusion limitation and substrate penetration in the biofilm [73,74]. The increase in biofilm thickness may lead to a more heterogeneous and biodiverse biofilm because of the stratification of metabolic processes and higher concentration gradient [75]. From Table 4, we can see higher ammonia removal was achieved with a thickness of 136.1  $\mu\text{m}$  by using a combination of nanobubble and coarse bubble aeration [59]. Thus, higher ammonia degradation may be achieved with an acceptable thickness of biofilm [76]. Excessive biofilm thickness will cause oxygen diffusion limitation, accumulate toxic metabolic by-products, and result in less active biomass in the deeper biofilm due to low oxygen penetration. Therefore, the microbial diversity decreases in less active biomass, consequently increasing the detachment from the deeper layer of the biofilm [77].

## 6. Conclusions

The recent study on bubble aeration system in biofilters for treatment of waste water in the RAS was reviewed. Nano, fine, medium, and coarse bubble aeration are used to oxygenate the biofilter in different scenarios. Oxygen transfer affects ammonia nitrogen oxidation and affects biofilter performance to remove contaminants from wastewater. Higher removal efficiency tends to result from finer bubble aeration. Approximately >80% TAN removal efficiency was achieved by the biofilter with an aeration system consisting of either fine, micro- and nanobubbles or a combination thereof. Furthermore, a higher volumetric mass transfer coefficient ( $k_L a_{(T)}$ ) resulted in higher oxygen transfer from bubbles to liquid media due to finer bubble aeration.

Based on the correlation between the microbial community and biofilm thickness due to different types of bubble aeration, it is concluded that the aeration system equipped with finer bubbles improves the ratio of nitrifying bacteria, and consequently, biofilm growth and thickness. Increasing biofilm thickness increases ammonia nitrogen removal in the system. However, it must be noted that the ammonia nitrogen removal decreases when an excessive thickness is formed, thereby limiting the diffusion of oxygen penetration into the deeper layer due to less active biomass.

**Author Contributions:** Conceptualization, I.M.J., F.F. and P.A.S.; methodology, P.A.S. and I.M.J.; review investigation, P.A.S.; data curation, P.A.S.; writing—original draft preparation, P.A.S.; writing—review and editing, I.M.J., F.F., C.P. and W.H.; supervision, I.M.J.; funding acquisition, I.M.J. All authors have read and agreed to the published version of the manuscript.

**Funding:** This research was funded by Academic Leadership Grant of Universitas Padjadjaran, grant number 2203/UN6.3.1/PT.00/2022 and The APC was funded by Universitas Padjadjaran.

**Data Availability Statement:** Not applicable.

**Acknowledgments:** The author acknowledges the scholarship given to Putu Ayustin Suriasni from Beasiswa Unggulan Pascasarjana Padjadjaran (BUPP) and this research also supported from Academic Leadership Grant with contract number no 2203/UN6.3.1/PT.00/2022.

**Conflicts of Interest:** The authors declare no conflict of interest.

## References

1. Deviller, G.; Aliaume, C.; Nava, M.A.F. High-rate algal pond treatment for water reuse in an integrated marine fish recirculating system: Effect on water quality and sea bass growth. *Aquaculture* **2004**, *235*, 331–344. [\[CrossRef\]](#)
2. Sánchez, O.I.A.; Matsumoto, T. Hydrodynamic characterization and performance evaluation of an aerobic three phase airlift fluidized bed reactor in a recirculation aquaculture system for Nile Tilapia production. *Aquac. Eng.* **2012**, *47*, 16–26. [\[CrossRef\]](#)
3. Cabasso, I. Membrane. In *Encyclopedia of Polymer Science and Engineering*; Wiley: New York, NY, USA, 1987; Volume 9, pp. 509–579.
4. Samer, M. Biological and Chemical Wastewater Treatment. In *Wastewater Treatment Engineering*; Intech: London, UK, 2015.
5. Holan, A.B.; Wold, P.-A.; Øie, G.; Leiknes, T.O. Integrated Membrane Bioreactor for Water Quality Control in Marine Recirculating Aquaculture Systems. *Sep. Sci. Technol.* **2013**, *48*, 1758–1767. [\[CrossRef\]](#)
6. Tasong, A.C.; Abao, R.P. Design and Development of an IoT Application with Visual Analytics for Water Consumption Monitoring. *Procedia Comput. Sci.* **2019**, *157*, 205–213. [\[CrossRef\]](#)
7. Malone, R.F.; Pfeiffer, T.J. Rating fixed film nitrifying biofilters used in recirculating aquaculture systems. *Aquac. Eng.* **2006**, *34*, 389–402. [\[CrossRef\]](#)
8. Ghangrekar, M.; Behera, M. Suspended Growth Treatment Processes. In *Comprehensive Water Quality and Purification*; Elsevier Inc.: Amsterdam, The Netherlands, 2014; pp. 75–89.
9. Gavrilescu, M.; Macoveanu, M. Attached-growth process engineering in wastewater treatment. *Bioprocess Biosyst. Eng.* **2000**, *23*, 95–106. [\[CrossRef\]](#)
10. Wang, X.; Xia, S.; Chen, L.; Zhao, J.; Renault, N.; Chovelon, J. Nutrients removal from municipal wastewater by chemical precipitation in a moving bed biofilm reactor. *Process. Biochem.* **2006**, *41*, 824–828. [\[CrossRef\]](#)
11. Roveto, P.M.; Schuler, A.J. Performance and diversity responses of nitrifying biofilms developed on varied materials and topographies to stepwise increases of aeration. *Bioresour. Technol.* **2019**, *281*, 429–439. [\[CrossRef\]](#)
12. Xiao, W.; Xu, G. Mass transfer of nanobubble aeration and its effect on biofilm growth: Microbial activity and structural properties. *Sci. Total Environ.* **2019**, *703*, 134976. [\[CrossRef\]](#)
13. Havlíček, K.; Nechanická, M.; Lederer, T.; Sirková, B.K. Analysis of nitrifying bacteria growth on two new types of biomass carrier using respirometry and molecular genetic methods. *Ecotoxicol. Environ. Saf.* **2021**, *225*, 112795. [\[CrossRef\]](#)
14. Tang, B.; Song, H.; Bin, L.; Huang, S.; Zhang, W.; Fu, F.; Zhao, Y.; Chen, Q. Determination of the profile of DO and its mass transferring coefficient in a biofilm reactor packed with semi-suspended bio-carriers. *Bioresour. Technol.* **2017**, *241*, 54–62. [\[CrossRef\]](#) [\[PubMed\]](#)
15. Liu, C.; Tang, Y. Application research of micro and nano bubbles in water pollution control. *E3S Web Conf.* **2019**, *136*, 06028. [\[CrossRef\]](#)
16. Ruen-ngam, D.; Wongsuchoto, P.; Limpanuphap, A.; Charinpanitku, T.; Pavasant, P. Influence of salinity on bubble size distribution and gas–liquid mass transfer in airlift contactors. *Chem. Eng. J.* **2008**, *141*, 222–232. [\[CrossRef\]](#)
17. Dias, J.; Bellingham, M.; Hassan, J.; Barrett, M.; Stephenson, T.; Soares, A. Influence of carrier media physical properties on start-up of moving attached growth systems. *Bioresour. Technol.* **2018**, *266*, 463–471. [\[CrossRef\]](#)
18. Kawan, J.A.; Suja, F.; Pramanik, S.K.; Yusof, A.; Rahman, R.A.; Hasan, H.A. Effect of Hydraulic Retention Time on the Performance of a Compact Moving Bed Biofilm Reactor for Effluent Polishing of Treated Sewage. *Water* **2022**, *14*, 81. [\[CrossRef\]](#)
19. Khuntia, S.; Majumder, S.K.; Ghosh, P. Microbubble-aided water and wastewater purification: A review. *Rev. Chem. Eng.* **2012**, *28*, 191–221. [\[CrossRef\]](#)
20. Sakr, M.; Mohamed, M.M.; Maraqa, M.A.; Hamouda, M.A.; Hassan, A.A.; Ali, J.; Jung, J. A critical review of the recent developments in micro–nano bubbles applications for domestic and industrial wastewater treatment. *Alex. Eng. J.* **2021**, *61*, 6591–6612. [\[CrossRef\]](#)
21. Shitu, A.; Liu, G.; Muhammad, A.I.; Zhang, Y.; Tadda, M.A.; Qi, W.; Liu, D.; Ye, Z.; Songming, Z. Recent advances in application of moving bed bioreactors for wastewater treatment from recirculating aquaculture systems: A review. *Aquac. Fish.* **2022**, *7*, 244–258. [\[CrossRef\]](#)
22. Ferreira, C.; Gonçalves, G. A Systematic Review on Life Extension Strategies in Industry. In Proceedings of the IEEE International Conference on Emerging Technologies and Factory Automation, ETFA, Vasteras, Sweden, 7–10 September 2021; Volume 10, pp. 1–17.
23. Hamza, R.A.; Iorhemen, O.T.; Tay, J.H. Advances in biological systems for the treatment of high-strength wastewater. *J. Water Process. Eng.* **2016**, *10*, 128–142. [\[CrossRef\]](#)
24. Reyes, A.A.D.; Lawson, T.B. Combination of a bead filter and rotating biological contactor in a recirculating fish culture system. *Aquac. Eng.* **1996**, *15*, 27–39. [\[CrossRef\]](#)
25. Kordkandi, S.A.; Khoshfetrat, A.B.; Faramarzi, A. Performance modelling of a partially-aerated submerged fixed-film bioreactor: Mechanistic analysis versus semi data-driven method. *J. Ind. Eng. Chem.* **2018**, *61*, 398–406. [\[CrossRef\]](#)

26. Jakobsen, H.A. Packed Bed Reactors. In *Chemical Reactor Modeling: Multiphase Reactive Flows*; Springer: Berlin/Heidelberg, Germany, 2008; pp. 953–984.
27. Liu, B.Y.M.; Pfeffer, J.T. *Modeling for Anaerobic Fixed-Bed Biofilm Reactors*; University of Illinois Urbana-Champaign: Champaign, IL, USA, 1989.
28. Malone, R.F. Floating Media Hourglass Biofilter. U.S. Patent 5,232,586, 3 August 1993.
29. Malone, R.F.; E Beecher, L. Use of floating bead filters to recondition recirculating waters in warmwater aquaculture production systems. *Aquac. Eng.* **2000**, *22*, 57–73. [\[CrossRef\]](#)
30. Wimberly, D.M. Development and Evaluation of a Low-Density Media Biofiltration Unit for Use in Recirculating Fish Culture Systems. Master's Thesis, Louisiana State University, Baton Rouge, LA, USA, 1990.
31. Ochoa, F.G.; Gomez, E. Bioreactor scale-up and oxygen transfer rate in microbial processes: An overview. *Biotechnol. Adv.* **2009**, *27*, 153–176. [\[CrossRef\]](#) [\[PubMed\]](#)
32. Xu, X.; Wei, W.; Liu, F.; Wei, W.; Liu, Z. Experimental study on aeration efficiency in a pilot-scale decelerated oxidation ditch equipped with fine bubble diffusers and impellers. *Can. J. Chem. Eng.* **2020**, *991*, 1410–1420. [\[CrossRef\]](#)
33. Kumar, A.; Moulick, S.; Mal, B. Design characteristics of pooled circular stepped cascade aeration system. *Aquac. Eng.* **2010**, *56*, 51–58. [\[CrossRef\]](#)
34. Pambudiarto, B.A.; Mindaryani, A.; Deendarlianto, D.; Budhijanto, W. Evaluation of the Effect of Operating Parameters on the Performance of Orifice/Porous Pipe Type Micro-bubble Generator. *J. Eng. Technol. Sci.* **2020**, *52*, 196–207. [\[CrossRef\]](#)
35. Takahashi, M.; Chiba, K.; Li, P. Free-Radical Generation from Collapsing Microbubbles in the Absence of a Dynamic Stimulus. *J. Phys. Chem. B* **2007**, *111*, 1343–1347. [\[CrossRef\]](#)
36. Ebina, K.; Shi, K.; Hirao, M. Oxygen and Air Nanobubble Water Solution Promote the Growth of Plants, Fishes, and Micer. *PLoS ONE* **2013**, *8*, e65339. [\[CrossRef\]](#) [\[PubMed\]](#)
37. ISO. *Fine Bubble Technology—General Principles for Usage and Measurement of Fine Bubbles—Part 1: Terminology*; ISO: Geneva, Switzerland, 2017.
38. Zăbavă, B.S.; Ungureanu, N.; Voicu, G.; Dincă, M. Types of Aerators Used in Wastewater Treatment Plants. In Proceedings of the 5th International Conference of Thermal Equipment, Renewable Energy and Rural Development, Golden Sands, Bulgaria, 2–4 June 2016.
39. Farmer, R.; Arndt, R. *Development of an Efficient Aeration System for Aquaculture*; University of Minnesota: Minneapolis, MN, USA, 1995.
40. Flemming, H.C.; Neu, T.R. The EPS matrix: The “house of biofilm cells”. *J. Bacteriol.* **2007**, *189*, 7945–7947. [\[CrossRef\]](#)
41. Karaguler, T.; Kahraman, H.; Tuter, M. Analyzing effects of ELF electromagnetic fields on removing bacterial biofilm. *Biocybern. Biomed. Eng.* **2017**, *37*, 336–340. [\[CrossRef\]](#)
42. Stoodley, P.; Sauer, K.; Davies, D.G.; Costerton, J.W. Biofilms as Complex Differentiated Communities. *Annu. Rev. Microbiol.* **2002**, *56*, 187–209. [\[CrossRef\]](#) [\[PubMed\]](#)
43. Goswami, S.; Sarkar, S.; Mazumder, D. A new approach for development of kinetics of wastewater treatment in aerobic biofilm reactor. *Appl. Water Sci.* **2016**, *7*, 2187–2193. [\[CrossRef\]](#)
44. Bouaifi, M.; Hebrard, G.; Bastoul, D.; Roustan, M. A comparative study of gas hold-up, bubble size, interfacial area and mass transfer coefficients in stirred gas-liquid reactors and bubble columns. *Chem. Eng. Process. Process Intensif.* **2001**, *40*, 97–111. [\[CrossRef\]](#)
45. Larsson, V. *Energy Savings with a New Aeration and Control System in a Mid-Size Swedish Wastewater Treatment Plant*; Uppsala University: Uppsala, Sweden, 2011.
46. Akita, K.; Yoshida, F. Bubble Size, Interfacial Area, and Liquid-Phase Mass Transfer Coefficient in Bubble Columns. *Ind. Eng. Chem. Process. Des. Dev.* **1974**, *13*, 84–91. [\[CrossRef\]](#)
47. Yao, G.-J.; Ren, J.-Q.; Zhou, F.; Liu, Y.-D.; Li, W. Micro-nano aeration is a promising alternative for achieving high-rate partial nitrification. *Sci. Total Environ.* **2021**, *795*, 148899. [\[CrossRef\]](#) [\[PubMed\]](#)
48. Woodard & Curran, Inc. Chapter 7—Methods for Treating Wastewaters from Industry. In *Industrial Waste Treatment Handbook*, 2nd ed.; Butterworth-Heinemann: Oxford, UK, 2006; pp. 149–334.
49. Liu, K.; Phillips, J.R.; Sun, X.; Mohammad, S.; Huhnke, R.L.; Atiyeh, H.K. Investigation and Modeling of Gas-Liquid Mass Transfer in a Sparged and Non-Sparged Continuous Stirred Tank Reactor with Potential Application in Syngas Fermentation. *Fermentation* **2019**, *5*, 75. [\[CrossRef\]](#)
50. Pfeiffer, T.J.; Wills, P.S. Evaluation of three types of structured floating plastic media in moving bed biofilters for total ammonia nitrogen removal in a low salinity hatchery recirculating aquaculture system. *Aquac. Eng.* **2011**, *45*, 51–59. [\[CrossRef\]](#)
51. Shitu, A.; Zhu, S.; Qi, W.; Tadda, M.A.; Liu, D.; Ye, Z. Performance of novel sponge biocarrier in MBBR treating recirculating aquaculture systems wastewater: Microbial community and kinetic study. *J. Environ. Manag.* **2020**, *275*, 111264. [\[CrossRef\]](#) [\[PubMed\]](#)
52. Summerfelt, S.T.; Zühlke, A.; Kolarevic, J.; Reiten, B.K.M.; Selset, R.; Gutierrez, X.; Terjesen, B.F. Effects of alkalinity on ammonia removal, carbon dioxide stripping, and system pH in semi-commercial scale water recirculating aquaculture systems operated with moving bed bioreactors. *Aquac. Eng.* **2015**, *65*, 46–54. [\[CrossRef\]](#)
53. Pfeiffer, T.J.; Riche, M.A. Evaluation of a Low-head Recirculating Aquaculture System Used for Rearing Florida Pompano to Market Size. *J. World Aquac. Soc.* **2011**, *42*, 198–208. [\[CrossRef\]](#)



54. Torno, J.; Einwächter, V.; Schroeder, J.P.; Schulz, C. Nitrate has a low impact on performance parameters and health status of ongrowing. *Aquaculture* **2018**, *489*, 21–27. [\[CrossRef\]](#)
55. Blancheton, J.P. Developments in recirculation systems for Mediterranean fish species. *Aquac. Eng.* **2000**, *22*, 17–31. [\[CrossRef\]](#)
56. Dosdat, A.; Ruyet, J.P.-L.; Covès, D.; Dutto, G.; Gasset, E.; Le Roux, A.; Lemarié, G. Effect of chronic exposure to ammonia on growth, food utilisation and metabolism of the European sea bass (*Dicentrarchus labrax*). *Aquat. Living Resour.* **2003**, *16*, 509–520. [\[CrossRef\]](#)
57. Albuquerque, A.; Makinia, J.; Pagilla, K. Impact of aeration conditions on the removal of low concentrations of nitrogen in a tertiary partially aerated biological filter. *Ecol. Eng.* **2012**, *44*, 44–52. [\[CrossRef\]](#)
58. Luo, G.; Xu, G.; Gao, J.; Tan, H. Effect of dissolved oxygen on nitrate removal using polycaprolactone as an organic carbon source and biofilm carrier in fixed-film denitrifying reactors. *J. Environ. Sci.* **2016**, *43*, 147–152. [\[CrossRef\]](#) [\[PubMed\]](#)
59. Xiao, W.; Xu, G.; Li, G. Role of shear stress in biological aerated filter with nanobubble aeration: Performance, biofilm structure and microbial community. *Bioresour. Technol.* **2021**, *325*. [\[CrossRef\]](#) [\[PubMed\]](#)
60. Shannon, C. A mathematical theory of communication. *Bell Syst. Tech. J.* **1948**, *27*, 379–423. [\[CrossRef\]](#)
61. Konopiński, M.K. Shannon diversity index: A call to replace the original Shannon's formula with unbiased estimator in the population genetics studies. *PeerJ* **2000**, *8*, e9391. [\[CrossRef\]](#)
62. Spohn, S.N.; Young, V.B. Gastrointestinal Microbial Ecology with Perspectives on Health and Disease. In *Physiology of the Gastrointestinal Tract*; Academic Press: Irvine, CA, USA, 2018; pp. 727–753.
63. Gonzalez-Silva, B.M.; Jonassen, K.R.; Bakke, I.; Østgaard, K.; Vadstein, O. Nitrification at different salinities: Biofilm community composition and physiological plasticity. *Water Res.* **2016**, *95*, 48–58. [\[CrossRef\]](#)
64. Bakke, I.; Åm, A.L.; Kolarevic, J.; Ytrestøyl, T.; Vadstein, O.; Attramadal, K.J.K.; Terjesen, B.F. Microbial community dynamics in semi-commercial RAS for production of Atlantic salmon post-smolts at different salinities. *Aquac. Eng.* **2016**, *78*, 42–49. [\[CrossRef\]](#)
65. Lee, J.; Kim, I.-S.; Emmanuel, A.; Koh, S.-C. Microbial valorization of solid wastes from a recirculating aquaculture system and the relevant microbial functions. *Aquac. Eng.* **2019**, *87*, 102016. [\[CrossRef\]](#)
66. Lee, D.-E.; Lee, J.; Kim, Y.-M.; Myeong, J.-I.; Kim, K.-H. Uncultured bacterial diversity in a seawater recirculating aquaculture system revealed by 16S rRNA gene amplicon sequencing. *J. Microbiol.* **2016**, *54*, 296–304. [\[CrossRef\]](#)
67. Ni, B.-J.; Yuan, Z. A model-based assessment of nitric oxide and nitrous oxide production in membrane-aerated autotrophic nitrogen removal biofilm systems. *J. Membr. Sci.* **2013**, *428*, 163–171. [\[CrossRef\]](#)
68. Michelin, M.; Mota, A.M.O.; Polizeli, M.L.T.M.; Silva, D.P.; Vicente, A.A.; Teixeira, J.A. Influence of volumetric oxygen transfer coefficient (kLa) on xylanases batch production by *Aspergillus niger* van Tieghem in stirred tank and internal-loop airlift bioreactors. *Biochem. Eng. J.* **2013**, *80*, 19–26. [\[CrossRef\]](#)
69. Fang, H.; Chen, Y.; Huang, L.; He, G. Analysis of biofilm bacterial communities under different shear stresses using size-fractionated sediment. *Sci. Rep.* **2017**, *7*, 1299. [\[CrossRef\]](#) [\[PubMed\]](#)
70. Agarwal, R.; Singh, S.; Bhilegaonkar, K.; Singh, V. Optimization of microtiter plate assay for the testing of biofilm formation ability in different *Salmonella* serotypes. *Int. Food Res. J.* **2011**, *18*, 1493–1498.
71. Gomes, I.B.; Meireles, A.; Gonçalves, A.L.; Goeres, D.M.; Sjollem, J.; Simões, L.C.; Simões, M. Standardized reactors for the study of medical biofilms: A review of the principles and latest modifications. *Crit. Rev. Biotechnol.* **2017**, *38*, 657–670. [\[CrossRef\]](#)
72. Gomes, L.C.; Moreira, J.M.; Teodósio, J.S.; Araújo, J.D.P.; Miranda, J.M. 96-well microtiter plates for biofouling simulation in biomedical settings. *Biofouling* **2014**, *30*, 535–546. [\[CrossRef\]](#)
73. Gapes, D.; Keller, J. Impact of oxygen mass transfer on nitrification reactions in suspended carrier reactor biofilms. *Process. Biochem.* **2009**, *44*, 43–53. [\[CrossRef\]](#)
74. Piculell, M.; Welander, P.; Jönsson, K.; Welander, T. Evaluating the effect of biofilm thickness on nitrification in moving bed biofilm reactors. *Environ. Technol.* **2015**, *37*, 732–743. [\[CrossRef\]](#)
75. Torresi, E.; Fowler, S.; Polesel, F.; Bester, K.; Andersen, H.; Smets, B.; Plósz, B.; Christensson, M. Biofilm thickness influences biodiversity in nitrifying MBBRs 1—Implications on micropollutant removal. *Environ. Sci. Technol.* **2016**, *50*, 9279–9288. [\[CrossRef\]](#) [\[PubMed\]](#)
76. Liu, Y.; Capdeville, B. Dynamics of nitrifying biofilm growth in biological nitrogen removal al process. *Water Sci. Technol.* **1994**, *29*, 377–380. [\[CrossRef\]](#)
77. Kumar, C.; Anand, S. Significance of microbial biofilms in food industry: A review. *Int. J. Food Microbiol.* **1998**, *42*, 9–27. [\[CrossRef\]](#) [\[PubMed\]](#)

**Disclaimer/Publisher's Note:** The statements, opinions and data contained in all publications are solely those of the individual author(s) and contributor(s) and not of MDPI and/or the editor(s). MDPI and/or the editor(s) disclaim responsibility for any injury to people or property resulting from any ideas, methods, instructions or products referred to in the content.